Chapter 7
Molecular Dynamics

7.1 Introduction

It is the aim of many branches of research in physics to describe macroscopic properties of matter on the basis of microscopic dynamics. However, a description of the simultaneous motion of a large number of interacting particles is in most cases not feasible by analytic methods. Moreover, a description is particularly difficult if the interaction between the particles is strong. Within the framework of statistical mechanics one tries to remedy these difficulties by employing some simplifying assumptions and by treating the system from a statistical point of view [1–4]. However, most of these simplifying assumptions are only justified within certain limits, such as the *weak coupling limit* or the *low density limit*. Nevertheless, it is not easy to establish how the solutions acquired are influenced by these limits and how the physics beyond these limits can be perceived. This makes the necessity of numerical solutions quite apparent. There are essentially two methods to determine physical quantities over a restricted set of states, namely *molecular dynamics* [5–7] and *Monte Carlo* methods. The technique of molecular dynamics will be discussed within this chapter while an introduction into some basic features of Monte Carlo algorithms is postponed to the second part of this book.

We strictly focus on a particular sub-field of molecular dynamics, namely on *classical molecular dynamics*, i.e. the treatment of classical physical systems. Extensions to quantum mechanical systems, which are commonly referred to as quantum molecular dynamics [8], will not be discussed here.

B.A. Stickler, E. Schachinger, *Basic Concepts in Computational Physics*,
DOI 10.1007/978-3-319-27265-8_7

7.2 Classical Molecular Dynamics

The classical model system for molecular dynamics consists of N particles with positions $r_i \equiv r_i(t)$, velocities $v_i \equiv v_i(t) = \dot{r}_i(t)$ and masses m_i, where $i = 1, 2, \ldots, N$. We note that r_i and v_i are vectors of the same dimension. We can write NEWTON's equations of motion as

$$m_i \ddot{r}_i = f_i(r_1, r_2, \ldots, r_N) \,, \tag{7.1}$$

where we introduced the forces $f_i \equiv f_i(r_1, r_2, \ldots, r_N)$. Again, we note that the forces f_i are vectors of the same dimension as r_i and v_i. We specify the forces f_i by demanding them to be *conservative*. Thus, we write

$$f_i(r_1, r_2, \ldots, r_N) = -\nabla_i U(r_1, r_2, \ldots, r_N) \,, \tag{7.2}$$

where ∇_i is the gradient pertaining to the spatial components of the i-th particle and $U(r_1, r_2, \ldots, r_N)$ is some potential which we will abbreviate by dropping its arguments: $U \equiv U(r_1, r_2, \ldots r_N)$. We then specify this potential U as the sum of two-particle interactions U_{ij} and some external potential U_{ext} as, for instance, the gravitational field or a static electric potential applied to the system:

$$U = \frac{1}{2} \sum_i \sum_{j \neq i} U_{ij} + U_{\text{ext}} \,. \tag{7.3}$$

In our discussion of the two-body problem (Appendix A) and, in particular, of the KEPLER problem in Chap. 4 we considered a central potential, which was proportional to $-1/r$. Due to the conservation of angular momentum, it was convenient to introduce an effective potential U_{eff} as the sum of an attractive and repulsive part as it was defined in Eq. (4.3) and illustrated in Fig. 4.1. In contrast, in molecular dynamics the most prominent two-body interaction potential is known as the LENNARD-JONES potential [9]. It is of the form

$$U(|r|) = 4\sigma \left[\left(\frac{\epsilon}{|r|} \right)^{12} - \left(\frac{\epsilon}{|r|} \right)^{6} \right] \,, \tag{7.4}$$

where ϵ and σ are real parameters and $|r|$ is the distance between two particles. The significance of the parameters ϵ and σ as well as the form of $U(|r|)$ defined by Eq. (7.4) is illustrated in Fig. 7.1. The LENNARD-JONES potential was particularly developed to model the interaction between neutral atoms or molecules. The repulsive term, which is proportional to $|r|^{-12}$, describes the PAULI repulsion while the attractive $|r|^{-6}$ term accounts for attractive VAN DER WAALS forces.

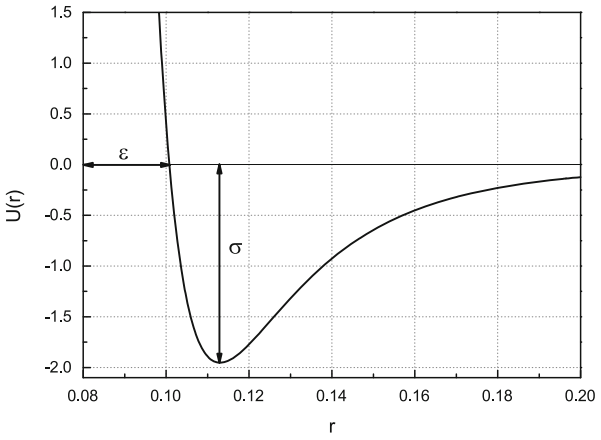

Fig. 7.1 Illustration of the LENNARD-JONES potential, Eq. (7.4). σ describes the depth of the potential well and ϵ is the position of the root of the LENNARD-JONES potential

We introduce the distance between particles i and j via

$$r_{ij} = |r_i - r_j| = |r_j - r_i| = r_{ji} \,, \tag{7.5}$$

and define the two-body potential

$$U_{ij} \equiv U(r_{ij}) \,, \tag{7.6}$$

where U is approximated by the LENNARD-JONES potential (7.4). Furthermore, we deduce from Eq. (7.4) that

$$f(|r|) = -\nabla_r U(|r|) = \frac{24\sigma}{|r|^2}\left[2\left(\frac{\epsilon}{|r|}\right)^{12} - \left(\frac{\epsilon}{|r|}\right)^{6}\right] r \,, \tag{7.7}$$

where we keep in mind that r is a vector. Hence, we write the forces f_i which appear in NEWTON's equations of motion (7.1) with the help of (7.3) in the form

$$\begin{aligned} f_i &= -\nabla_i U \\ &= -\nabla_i \left(\frac{1}{2}\sum_k \sum_{l\neq k} U_{kl} + U_{\text{ext}}\right) \\ &= -\sum_{j\neq i} \nabla_i U_{ij} - \nabla_i U_{\text{ext}} \\ &= \sum_{j\neq i} f(r_{ij}) + f^i_{\text{ext}} \\ &= \sum_{j\neq i} f_{ij} + f^i_{\text{ext}} \,, \end{aligned} \tag{7.8}$$

where we implicitly defined the external force f^i_{ext} acting on particle i and the two-particle forces f_{ij} acting between particle i and j. We want to make the road visible, which guides us to a numerical solution of NEWTON's equations of motion (7.1), and introduce the vectors $R = (r_1, r_2, \ldots, r_N)^T$, $V = (v_1, v_2, \ldots, v_N)^T = \dot{R}$, and $F = (f_1/m_1, f_2/m_2, \ldots, f_N/m_N)^T$. This transforms Eq. (7.1) into the very compact form

$$\ddot{R} = F \,, \tag{7.9}$$

which is equivalent to a set of two first order ordinary differential equations:

$$\begin{pmatrix} \dot{R} \\ \dot{V} \end{pmatrix} = \begin{pmatrix} V \\ F \end{pmatrix} \,. \tag{7.10}$$

This set is already of the standard form (5.1) of initial value problems.

We are now in a position to proceed with a discussion of some numerical methods which have been developed in Chap. 5 to solve this initial value problem. For this sake, we regard discrete time instances $t_k = k\Delta t$, where $k \in \mathbb{N}$ and function values at these discrete time instances t_k are denoted by a subscript k, as for instance $R_k \equiv R(t_k)$.

(i) In a first approximation we apply the symplectic EULER method [see Eq. (4.33)] to Eq. (7.10) and obtain

$$\begin{pmatrix} R_{k+1} \\ V_{k+1} \end{pmatrix} = \begin{pmatrix} R_k \\ V_k \end{pmatrix} + \begin{pmatrix} V_{k+1} \\ F_k \end{pmatrix} \Delta t \,. \tag{7.11}$$

Inserting the second into the first equation results in

$$R_{k+1} = R_k + V_k \Delta t + F_k \Delta t^2 \,. \tag{7.12}$$

The velocity V_k at time t_k is then approximated by the backward difference derivative (2.10b) and we find the recursion relation:

$$R_{k+1} = 2R_k - R_{k-1} + F_k \Delta t^2 \,. \tag{7.13}$$

We note that it is only valid for $k \geq 1$. The initialization step necessary to complete the analysis is found by expanding R_1 in a TAYLOR series up to second order:

$$R_1 = R_0 + \Delta t V_0 + \frac{1}{2} F_0 \Delta t^2 \,. \tag{7.14}$$

This method is referred to as the STÖRMER-VERLET algorithm [10]. Note that Eq. (7.14) serves as the initialization of the sequence of time steps.

Furthermore, we remark that Eq. (7.13) could have also been obtained using the central difference derivative to approximate the second time derivative in Eq. (7.1):

$$\ddot{R}_k \approx \frac{R_{k+1} - 2R_k + R_{k-1}}{\Delta t^2} = F_k \,. \tag{7.15}$$

In summary, the VERLET or STÖRMER-VERLET algorithm is defined by the following set of equations:

$$\begin{aligned} R_{k+1} &= 2R_k - R_{k-1} + F_k \Delta t^2 \,, \qquad k \geq 1, \\ R_1 &= R_0 + \Delta t V_0 + \frac{1}{2} F_0 \Delta t^2 \,. \end{aligned} \tag{7.16}$$

(ii) We employ the central rectangular rule of integration (Sect. 3.2) in order to obtain approximations which are formally equivalent to Eq. (5.11). In particular, we obtain from Eq. (7.10):

$$R_{k+1} = R_k + V_{k+\frac{1}{2}} \Delta t \,. \tag{7.17}$$

We note that the value of $V_{k+1/2}$ is yet undetermined. However, it can be determined in a similar fashion via

$$V_{k+\frac{1}{2}} = V_{k-\frac{1}{2}} + F_k \Delta t \,. \tag{7.18}$$

This method is referred to as the *leap-frog* algorithm and is initialized by the relation

$$V_{\frac{1}{2}} = V_0 + \frac{\Delta t}{2} F_0 \,. \tag{7.19}$$

This equation can also be obtained by expanding $V_{1/2}$ in a TAYLOR series up to first order around the point $t_0 = 0$ and by noting that $\dot{V}_k = F_k$. In summary we write the leap-frog algorithm as

$$\begin{aligned} R_{k+1} &= R_k + V_{k+\frac{1}{2}} \Delta t \,, \\ V_{k+\frac{1}{2}} &= V_{k-\frac{1}{2}} + F_k \Delta t \,, \\ V_{\frac{1}{2}} &= V_0 + \frac{1}{2} F_0 \Delta t \,. \end{aligned} \tag{7.20}$$

(iii) A third, very elegant alternative is the so-called *velocity* VERLET algorithm. We expand R_{k+1}:

$$R_{k+1} = R_k + V_k \Delta t + \frac{1}{2} F_k \Delta t^2 \,. \tag{7.21}$$

This allows to calculate the spatial coordinates at time t_{k+1} if R_k and V_k are given. Note that $F_k \equiv F(R_k)$ is completely determined by the positions R_k. Nevertheless, we need one more relation in order to determine the velocities at times t_{k+1}. Again, we expand V_{k+1} in a TAYLOR series. However, we approximate the remainder by the arithmetic mean between t_k and t_{k+1}:

$$V_{k+1} = V_k + \frac{1}{2} \left(F_k + F_{k+1} \right) \Delta t \,. \tag{7.22}$$

The strategy is clear: we calculate the positions R_{k+1} from Eq. (7.21) for given values of R_k and V_k. With the help of R_{k+1} we compute F_{k+1}, which is then inserted into Eq. (7.22) which determines V_{k+1}. In summary, the complete algorithm of the velocity VERLET method is defined by the steps:

$$\begin{aligned} R_{k+1} &= R_k + V_k \Delta t + \frac{1}{2} F_k \Delta t^2 \,, \\ V_{k+1} &= V_k + \frac{1}{2} \left(F_k + F_{k+1} \right) \Delta t \,. \end{aligned} \tag{7.23}$$

We note some properties of these methods. The STÖRMER-VERLET algorithm of Eq. (7.16) is time-reversal symmetric (invariant under the transformation $\Delta t \to -\Delta t$), hence reversible. This is a direct consequence of its relation to the symplectic EULER method. Moreover, the positions R_k obtained with this method are highly accurate, however, the procedure suffers under an inaccurate approximation of the velocities V_k. This shortcoming is clearly remedied by the leap-frog algorithm (7.20) or the velocity VERLET algorithm (7.23). However, these methods are not time-reversal invariant. Hence, one has to decide whether or not very accurate values for the velocities are required for the problem at hand. In many cases the velocity VERLET algorithm is the most popular choice.

7.3 Numerical Implementation

The rough structure of a molecular dynamics code consists of three crucial steps, namely

- Initialization,
- start simulation and equilibrate,
- continue simulation and store results.

In the following we discuss some of the most important subtleties associated with these three parts. In particular we will focus on the choice of appropriate boundary conditions and on the choice of the scales of characteristic quantities.

Boundary Conditions

Basically, there are two possibilities: (i) The system is of finite size and the implementation of boundary conditions might be straightforward. For instance, let us assume that we regard N particles within a finite box of reflecting boundaries, we simply propagate the particle-coordinates in time and if a particle tries to leave the box, we correct its trajectory according to a reflection law. The velocity is adjusted accordingly. This is illustrated in Fig. 7.2 for a two-dimensional case and the particular situation that the particle is reflected from the right hand boundary of the box. The corresponding equations read

$$r_{k+1} = \begin{pmatrix} x_{k+1} \\ y_{k+1} \end{pmatrix} = \begin{pmatrix} L - (\tilde{x}_{k+1} - L) \\ \tilde{y}_{k+1} \end{pmatrix} , \tag{7.24}$$

and

$$v_{k+1} = \begin{pmatrix} v_{k+1,x} \\ v_{k+1,y} \end{pmatrix} = \begin{pmatrix} -\tilde{v}_{k+1,x} \\ \tilde{v}_{k+1,y} \end{pmatrix} . \tag{7.25}$$

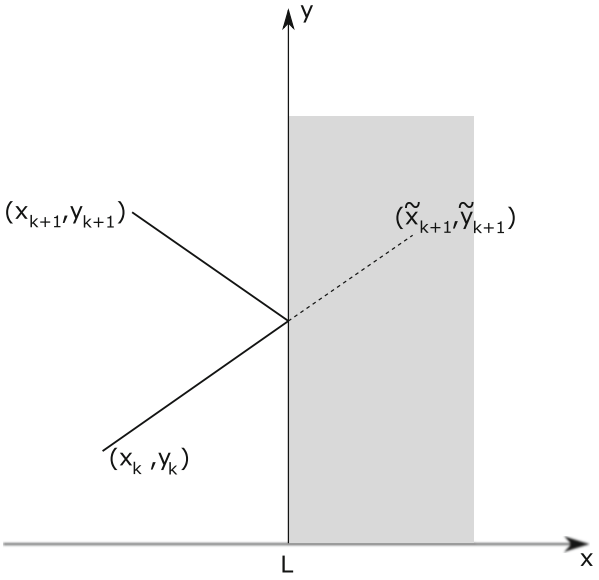

Fig. 7.2 Illustration of the reflection principle for a box of finite dimension with reflecting boundaries

Here, L denotes the length of the box and $\tilde{x}_{k+1}$, $\tilde{y}_{k+1}$, $\tilde{v}_{k+1,x}$ and $\tilde{v}_{k+1,y}$ are the positions and velocities one would have obtained in the absence of the boundary, see Fig. 7.2.

(ii) The system is not confined. Then the situation is entirely different. Of course, one could approximate the infinite volume by a large but finite volume. In such a case the influence of a constraint to finite size is usually not negligible. The induced errors are referred to as *finite volume effects*. A very popular choice are so called *periodic boundary conditions* which means that a finite system is surrounded by an infinite number of completely identical replicas of the system, where the forces are allowed to act across the boundaries. Because of this, calculating the force on one particle requires the evaluation of an infinite sum. This is numerically not manageable and we have to find ways to truncate the sum. For instance, it might be a good approximation to restrict the sum to nearest-neighbor cells. However, the applicability of such an approach highly depends on the properties of the system under investigation and, in particular, on the range of the interaction potential. In case of a LENNARD-JONES potential the quantity defining the range of the interaction potential is ϵ, see Fig. 7.1.

If a particle leaves the box, it enters the box at the same time on the opposite side. More generally, due to the requirement of identical replicas, we have for all observables $O(r)$ that $O(r + nK) = O(r)$, where r lies within the central box, K is a lattice vector pointing to one of the neighboring cells and $n \in \mathbb{Z}$.

There is another crucial point concerning periodic boundary conditions. In case of a closed system, the system is definitely at rest. However, if periodic boundary conditions are imposed it is possible that the particles move with constant velocity from one cell to another, which, in our case, resembles circling trajectories. This is definitely not desirable since the total velocity is a measure of the kinetic energy and, therefore, of the temperature of the system. However, one can *shift* the total velocity in order to remedy this problem. In particular, if

$$v_{\text{tot}} = \sum_{i=1}^{N} v_i \neq 0 \,, \tag{7.26}$$

the shift

$$v_i' = v_i - \frac{1}{N} v_{\text{tot}} \,, \tag{7.27}$$

yields the desired result. We note that in a case where all masses are identical, i.e. $m_1 = m_2 = \ldots = m_N \equiv m$, this is equivalent to $p_{\text{tot}} = m v_{\text{tot}} = 0$.

In conclusion, we remark that the choice of boundary conditions is not the only item to be considered in the definition of the system. Another quite crucial point might be the size of the box. If an infinite system is modeled using finite systems, the dimension of the box *must* fairly exceed the mean free path of the particles. Otherwise, the influence of the boundaries is going to perturb significantly the outcome of the numerical experiment.

Initialization and Equilibration

We remember from statistical physics [1–4] that every degree of freedom in the system (7.1) contributes just $k_B T/2$ to the total kinetic energy because of the equipartition theorem. Here k_B is BOLTZMANN's constant and T is the temperature. If we regard N particles, which move in a d-dimensional space, we have $d(N-1)$ degrees of freedom, if we demand that $v_{tot} = 0$. Hence, we have

$$E_{kin} = \frac{1}{2} \sum_{i=1}^{N} m_i v_i^2 = \frac{d(N-1)}{2} k_B T \,, \tag{7.28}$$

which gives a relation from which we can determine the temperature of the system:

$$k_B T = \frac{1}{d(N-1)} \sum_{i=1}^{N} m_i v_i^2 \,. \tag{7.29}$$

However, in many applications the system is supposed to be simulated at a *given* temperature, i.e. the temperature T is an input rather than an output parameter and is supposed to stay constant during the simulation. We can control the temperature by rescaling the velocities and this might be necessary at several times during the simulation in order to guarantee a constant temperature. We define

$$v_i' = \lambda v_i \,, \tag{7.30}$$

where λ is a rescaling parameter. The temperature associated with the velocities v_i' is given by

$$k_B T' = \frac{\lambda^2}{d(N-1)} \sum_{i=1}^{N} m_i v_i^2 \,. \tag{7.31}$$

This allows to determine how to choose λ in order to obtain a certain temperature T':

$$\lambda = \sqrt{\frac{d(N-1)k_B T'}{2E_{kin}}} \,. \tag{7.32}$$

We note that if the total velocity, which is the sum of all velocities v_i, is zero, the total velocity corresponding to the rescaled velocities v_i' is also equal to zero since

$$\sum_{i=1}^{N} v_i' = \lambda \sum_{i=1}^{N} v_i = 0 \,. \tag{7.33}$$

This ensures that rescaling of the velocities does not induce a bias.

The choice of the initial conditions highly influences the time the system needs to reach thermal equilibrium. For instance, if a gas is to be simulated at a given temperature T it might be advantageous to choose the initial velocities according to a MAXWELL-BOLTZMANN distribution. The MAXWELL-BOLTZMANN distribution states that the probability [more precisely: the pdf (*probability density function* describing the probability, see Appendix E)] that a particle with mass m has velocity v is proportional to

$$p(|v|) \propto |v|^2 \exp\left(-\frac{m|v|^2}{2k_\mathrm{B}T}\right) . \tag{7.34}$$

Another intriguing question is how to check whether or not thermal equilibrium has been reached. In statistical mechanics one is usually confronted with expectation values of observables $O(t)$ as a function of time. The expectation value $\langle O \rangle$ is defined as

$$\langle O \rangle = \lim_{\tau \to \infty} \frac{1}{\tau} \int_0^\tau \mathrm{d}t O(t) . \tag{7.35}$$

Since $O(t)$ is not known analytically one replaces the mean value by its arithmetic mean

$$\langle O \rangle \approx \overline{O} = \frac{1}{n} \sum_{j=k+1}^{k+n} O(t_j) . \tag{7.36}$$

If n and k are sufficiently large, the average value can be regarded as converged. In particular, one has to choose n reasonably large and then find k in such a way, that for all values $k' \geq k$ the same result for $\overline{O}$ is obtained. Hence, equilibrium has been reached after k time-steps and it is now possible to 'measure' the observables by calculating their mean values. A more detailed discussion of such a procedure, as, for instance, the influence of time correlations or a discussion of more advanced techniques is postponed to Chap. 19.

There is one last point: In many cases the *natural units* of the physical system might be disadvantageous because they are likely to induce numerical instabilities. In such cases a common technique is to switch to *rescaled variables* by introducing new units, which are characteristic quantities for the system and all physical quantities are expressed in these new units. For instance one might introduce the length L of the box as the unit of space. The new spatial coordinates would then be given by

$$r' = \frac{r}{L} . \tag{7.37}$$

Hence all coordinates take on values within the interval $r' \in [0, 1]$. However, one cannot introduce an arbitrary set of characteristic quantities due to the physical relations they have to obey. For instance, one might introduce a characteristic energy E_0, a characteristic length λ, and a characteristic mass m. In this case the characteristic temperature $\tilde{T}$ is determined via

$$\tilde{T} = \frac{E_0}{k_B} . \tag{7.38}$$

Moreover the characteristic time τ is fixed to the value

$$\tau = \sqrt{\frac{m\lambda^2}{E_0}} , \tag{7.39}$$

which results from the relation between the kinetic energy and the velocity.

To illustrate a molecular dynamics simulation we study a set of $N = 100$ particles of mass $m = 1$ which are subject to a LENNARD-JONES potential (7.4) characterized by $\epsilon = \sigma = 1$ and to a gravitational force mg, $g = 9.81$. At initialization the particles are placed in a 10×10 lattice starting with the lower left hand edge at $x = 10.5$ and $y = 10$. The particles are equally spaced with $\Delta x = \Delta y = \epsilon$. This initial configuration is shown in Fig. 7.3a. Furthermore, the left hand side, the right hand side, and the bottom of the confinement ($L = 30$) are described by reflecting boundary conditions, Eqs. (7.24) and (7.25). The confinement is open at the top, i.e. it extends to infinity. The time step is given by $\Delta t = 10^{-3}$. Figure 7.3b–d demonstrate how the system developed after 1200, 1800, and 3000 time steps, respectively.

This chapter closes our discussion of the numerics of initial value problems. In the following chapters we will introduce some of the basic concepts developed to solve boundary value problems with numerical methods.

Summary

This chapter dealt with the classical dynamics of many particles (not necessarily identical particles) which are confined in a box of finite dimension or which are allowed to roam freely in infinite space. The particles are subject to a particle-particle interaction and to an external force. The discussion was restricted to classical molecular dynamics. From NEWTON's equations of motion for N interacting particles numerical methods were developed which allowed the simulation of the particles' dynamics. Based on the symplectic EULER method the STÖRMER-VERLET algorithm was derived. Another approach was based on the central rectangular rule and resulted in the *leap-frog* algorithm. Finally, the *velocity* VERLET algorithm was introduced. All three methods do have their merits. The first gives very accurate results for the particles' positions but calculates inaccurate

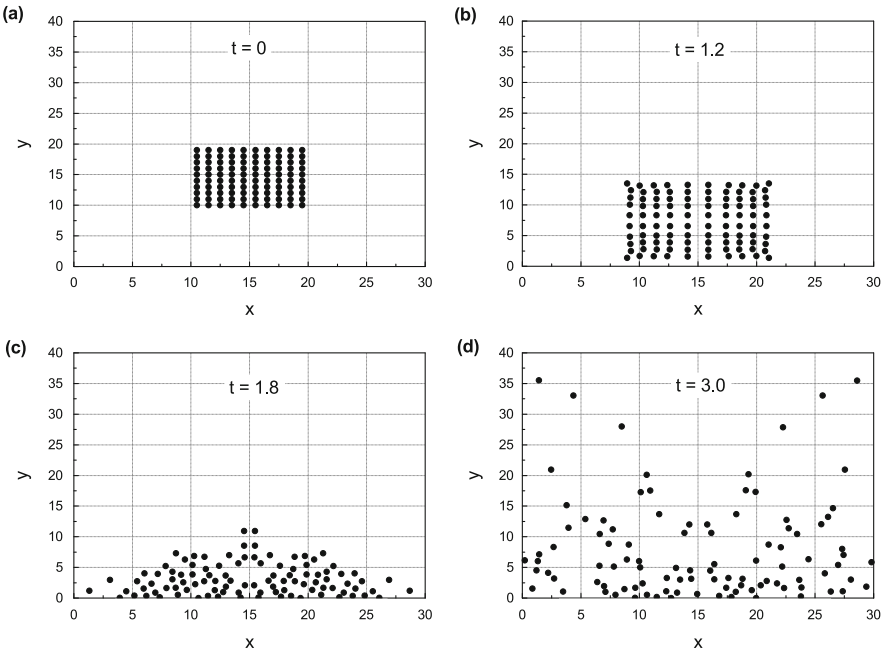

Fig. 7.3 **(a)** Initial configuration: the particles are placed in a 10×10 equally spaced lattice starting with $x = 10.5$ and $y = 10.0$; $g = 9.81$. The initial velocities are equal to zero. **(b)** Configuration after 1200 time steps. **(c)** Configuration after 1800 time steps. **(d)** Configuration after 3000 time steps

velocities. It has the advantage that it is time reversible. The other two methods lack this property but give very accurate estimates of the particles' velocities. The final part of this chapter was dedicated to the discussion of various subtleties of the numerical implementation of these algorithms as there were: (i) definition of boundary conditions, (ii) initialization of the algorithm, (iii) equilibration to a given temperature, (iv) ensuring constant temperature throughout the simulation, and (v) transformation to rescaled variables.

Problems

1. We investigate the pendulum of Chap. 1 and write its equation of motion as

$$\ddot{x} + \omega^2 x = 0 \,,$$

with $\omega = \sqrt{g/\ell}$. The STÖRMER-VERLET algorithm is applied to simulate the pendulum's motion and to compare the numerical results with the exact solution.

Demonstrate that the result is very sensitive to the choice of the time step Δt and, in particular, of the product $\omega \Delta t$. Note that in this particular case the STÖRMER-VERLET algorithm can also be studied analytically! What happens for the choice $\omega \Delta t = 1$ or $\omega \Delta t \geq 2$? Which conclusions can be drawn from this example for a proper choice of the time discretization?

Try the other two methods to simulate the pendulum's dynamics.

2. Write a molecular dynamics code with the help of the following instructions. You can use either the leap-frog or the velocity VERLET algorithm. We consider the following system:

   - There are $N = 100$ particles in a two-dimensional box with side length $L = 30$. The boundaries at the bottom, at the left- and at right-hand side are considered as reflecting, as in Fig. 7.2. The top of the box is regarded as open (no periodic boundary condition or reflecting boundary is imposed).
   - The particles interact through a LENNARD-JONES potential of the form (7.4) where ϵ and σ define the interaction.
   - Furthermore, a gravitational force $F_{\text{ext}} = -mge_y$ acts on each particle, where m is the particle's mass, g is the acceleration due to gravity, and e_y denotes the unit vector in y-direction.
   - As an initial condition, the particles can be placed within the box on a regular lattice, where the distance between the particles is the characteristic distance according to the LENNARD-JONES potential, i.e. ϵ. The form and position of this lattice is arbitrary. This is illustrated in Fig. 7.3.

   We measure the velocities and the positions of all particles. Since the particle's velocities and positions are to be analyzed with the help of an extra program, the data are written to external files (it is not necessary to save *all* time steps!).

   Perform the following analysis:

   - Determine the temperature T from the kinetic energy as discussed in in this chapter. Note that in this particular case we do not demand that $v_{tot} = 0$!
   - Try different initial conditions. For instance, set the initial velocity equal to zero and stack the particles in different geometric configurations (rectangle, triangle, ..., one can also use more than one configurations at the same time!). The nearest neighbor distance between the particles can be set equal to ϵ. Choose one configuration and place it at different positions in the box. What happens?
   - Set $\epsilon = \sigma = m = 1$ (we change the units) and set in the initial condition to the inter-atomic distance of $2^{\frac{1}{6}}\epsilon$. (Why?) Vary the gravitational acceleration g (different systems of units) in order to simulate different states of matter. The reference program developed solid behavior for $g \approx 0$, liquid behavior for $g \approx 0.1$ and gaseous behavior for $g > 1$. Explain this behavior!
   - Measure the particle density $\rho(h)$ as a function of the height h. You should be able to reproduce the barometric formula:

$$\rho \propto \rho_0 \exp\{-\gamma h/T\}, \quad \gamma > 0 \, .$$

- Determine the momentum distribution ($p_i = mv_i$) of the particles and demonstrate that it follows a MAXWELL-BOLTZMANN distribution

$$p(|v|) \propto |v|^2 \exp\{-\gamma |v|^2/T\}\,, \quad \gamma > 0\,,$$

  with $|v| = \sqrt{v_x^2 + v_y^2}$, the Euclidean norm.
- Illustrate the results of the simulation graphically.

References

1. Mandl, F.: Statistical Physics, 2nd edn. Wiley, New York (1988)
2. Schwabl, F.: Statistical Mechanics. Advanced Texts in Physics. Springer, Berlin/Heidelberg (2006)
3. Halley, J.W.: Statistical Mechanics. Cambridge University Press, Cambridge (2006)
4. Hardy, R.J., Binek, C.: Thermodynamics and Statistical Mechanics: An Integrated Approach. Wiley, New York (2014)
5. Hoover, W.G.: Molecular Dynamics. Springer, Berlin/Heidelberg (1986)
6. Griebel, M., Knapek, S., Zumbesch, G.: Numerical Simulation in Molecular Dynamics. Texts in Computational Science and Engeneering, vol. 5. Springer, Berlin/Heidelberg (2007)
7. Marx, D., Hutter, J.: Ab Initio Molecular Dynamics. Cambridge University Press, Cambridge (2012)
8. Gatti, F. (ed.): Molecular Quantum Dynamics. Springer, Berlin/Heidelberg (2014)
9. Jones, J.E.: On the determination of molecular fields. II. From the equation of state of a gas. Proc. R. Soc. A **106**, 463–477 (1924). doi:10.1098/rspa.1924.0082
10. Hairer, E., Lubich, C., Wanner, G.: Geometric numerical integration illustrated by the Störmer-Verlet method. Acta Numer. **12**, 399–450 (2003). doi:10.1017/S0962492902000144